# OpenFOAM validation for indoor ventilation applications

João M. Miranda[1], Guilherme Osswald[1], Fernando A. Castro[1], Rui A. Rego[1,2]

[1]*LAVAC-DEM, ISEP, Polytechnic of Porto*
*R. Dr. António Bernardino de Almeida, 4249-015, Porto, Portugal*
*1170733@isep.ipp.pt, 1170563@isep.ipp.pt, fac@isep.ipp.pt, RFR@isep.ipp.pt*
[2]*M4S, ISEP, Polytechnic of Porto*
*R. Dr. António Bernardino de Almeida, 4249-015, Porto, Portugal*
*RFR@isep.ipp.pt*

**Abstract.** The use of Computational Fluid Dynamics (CFD) to study ventilation strategies in indoor spaces is an crucial tool for energy consumption reduction and sustainability. In this study, the application of several turbulence models for indoor ventilation modelling were validated using the OpenFOAM software. These validations were based on two experimental benchmark cases available in the literature. In the first case, an isothermal quasi 2-dimensional flow in a room with one inlet and one outlet was studied. Comparisons of URaNS simulations using the `pimpleFoam` solver together with the high-Reynolds number $k-\epsilon$, RNG $k-\epsilon$ and the low-Reynolds number LaunderSharma $k-\epsilon$ and $k-\omega SST$ turbulence models are presented. The second benchmark case is a three-dimensional non-isothermal flow in a room with one inlet (cold jet) and four outlets placed in a vertical opposite wall, where a heat flux is applied. The flow has an Archimedes number of 0.016. For the second case URaNS simulations were performed using the `buoyantPimpleFoam` solver with $k-\epsilon$ turbulence model with buoyant production term, and the isothermal $k-\epsilon$ and RNG $k-\epsilon$ turbulence models. In the first benchmark case all turbulence models produced a good description of the experimental flow with exception of $k-\omega SST$ that overestimated the size of the recirculating zone and was then discarded from further tests. The second benchmark case, performed only with high-Reynolds number turbulence models, showed an overall good agreement with the experimental results, and, as almost expected, the buoyant $k-\epsilon$ model had the best performance pointing the importance of the buoyant term inclusion on other popular turbulence models of the OpenFOAM library.

**Keywords:** HVAC, CFD Validation, OpenFOAM, URaNS

## 1 Introduction

The buildings sector is responsible for about one third of total energy consumption, which is reflected in 28% of all $CO_2$ emissions released into the atmosphere (2021 data).The Heating, Ventilation and Air Conditioning (HVAC) systems account for around 38% of all buildings consumption, which is equivalent to 12% of the total energy consumed (González-Torres et al. [1]). Thus, HVAC systems reduction of energy consumption and optimisation is a good way to improve sustainability and reduce emissions.

One tool that has been evolving since the 70's in the HVAC area, with the initial works of Nielsen [2], Restivo [3] and with a great potential to help designers to reduce the energy and emissions of the HVAC systems, is the energy and flow simulation based on Computational Fluid Dynamics (CFD). Herein, one will restrain to the Unsteady Reynolds-Averaged Navier-Stokes (URaNS) formulation for dealing with time dependent flow.

In this work the main objective is to further add to the work of Almeida [4] in regard to validation of a numerical simulation tool for the study of air distribution in rooms. For that purpose, one used the OpenFOAM software in the simulation of two well know experimental benchmarks.

The first studied case is the classic benchmark, IEA Annex 20, from Nielsen [2], one inlet and one outlet quasi 2-dimensional flow. This case has been used as a isothermal validation case by several authors, namely Ito et al. [5], Rong and Nielsen [6], Elhadidi and Khalifa [7] and Almeida [4].

The second benchmark case was the study of Murakami et al. [8], which was developed to analyze a non-

isothermal case, since, according to the author, "air-conditioned rooms are generally not isothermal, and the buoyancy force caused by the temperature difference exerts a non-negligible effect not only in the mean flow, but also in its turbulence properties"(Murakami et al. [8], p.11, author's translation). Other studies already carried out for this case can be found in Ito et al. [5] and Murakami et al. [9].

## 2 Isothermal Annex 20 case study (3D)

The first validation task consisted in the numerical simulation of the Annex 20 case of Nielsen [2], an isothermal flow in a room whose geometry is presented in Fig. 1a. The room, with one inlet and one outlet, is characterised by the dimensions h = 0.168 m, t = 0.48 m, H = 3.0 m, L = 9.0 m and W = 3.0 m. In Nielsen [2] the room was operated with an inflow of air at 20ºC ($\nu = 1.51 \times 10^{-5}$ m$^2$/s), producing a $Re_h = \frac{hU_0}{\nu} \approx 5000$ at the inlet ($U_0 = 0.455$ m/s) and experimental results were obtained with laser-doppler measurements at the inlet slot and along the lines presented in Fig. 1b, both at the y/W=0.5 (symmetry plane) and at y/W=2.7.

In this study, two higth-Reynolds number turbulence models ($k-\epsilon$ and RNG $k-\epsilon$) and two low-Reynolds number turbulence models (LaunderSharma $k-\epsilon$ and $k-\omega SST$) were used with the OpenFOAM `pimpleFoam` solver, which is an incompressible and transient solver for isothermal flows. All simulations in this section were performed using the `upwind` convection scheme. See OpenCFD [10], [11], Greenshields and Weller [12] for further details of models and solvers.

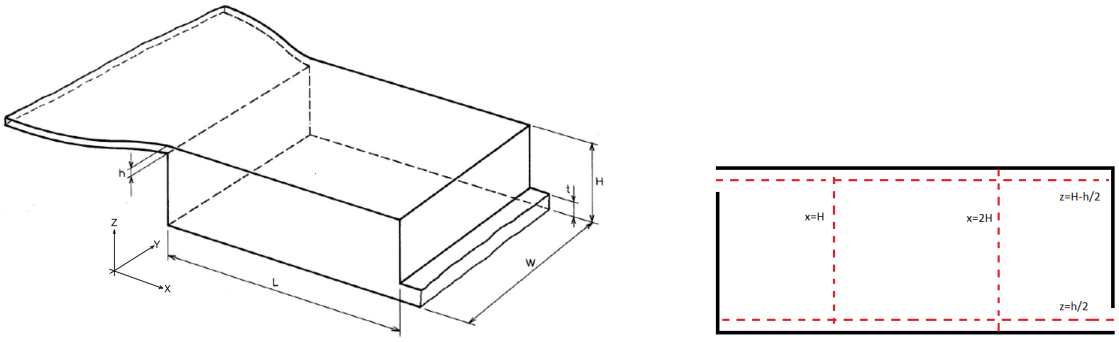


(a) (b)

Figure 1. Annex 20; (a) room geometry schematic; (b) measurement zones.

### 2.1 Supply channel

To obtain the inlet conditions for the room, for the mean and turbulent fields, precursor simulations were performed in a channel with the same cross sectional area of the inlet slot and with a longitudinal length of 0.3 m. These simulations used periodic boundary conditions in the longitudinal direction, implemented with the help of the `meanVelocityForce` type of `momentumSource` that can be configured in the OpenFOAM `fvOptions` file.

Several meshes of increasing grid density were tested until mesh independence was achieved, that occurred for meshes with over $31 \times 65 \times 120$ grid nodes in the x, y and z directions, respectively. Simulations were carried out until reaching the steady state, observable in the time series of the calculation variables. Numerical results obtained using the aforementioned mesh and the four turbulence models are presented in Fig. 2, together with the experimental results (all at the symmetry plane).

All turbulence models overestimated both the mean and turbulent fields, as can bee seen in the profiles of Fig. 2. This seems to be a recurrent problem when trying to use channel flow simulations to produce the Annex 20 inlet boundary, as is for example the case of Almeida [4], that used a long channel section attached to the room geometry to allow for flow development from uniform flow conditions placed at the upstream boundary. Besides numerical techniques and turbulence model limitations the fact that the actual inlet duct induces flow acceleration, because of the convergent profile, it will contribute to produce a flatter velocity profile at the core of the experimental cross section, as can be seen e.g. in Goltsman et al. [13]. Also, the acceleration of the flow has a stabilising effect, resulting in a reduction of the turbulent activity (see e.g. Pope [14]), possibly justifying the reduced turbulent intensity in the experimental results.

Globally, the two low-Reynolds number turbulent models produced the best results.

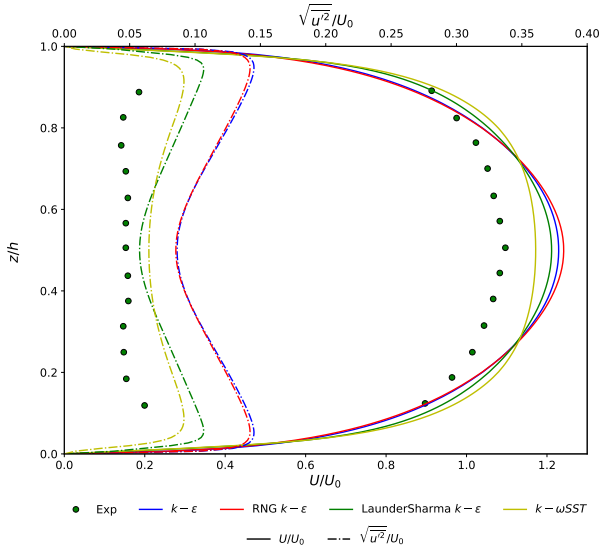


Figure 2. Comparison of the channel profile between the experimentally measured values taken from Nielsen [2] and the different simulated turbulence models, for the symmetry plane ($W = 1.5$ m)

### 2.2 Annex 20 room

The steady state results obtained from the supply channel, presented previously, were used to implement the inlet boundary condition for the room simulations. Numerical results for a cross section of the channel were used together with the `timeVaryingMappedFixedValue` function to implement the steady state inlet condition for the room simulations to all variables except pressure. Besides a possible temporal interpolation, that was not used here, the `timeVaryingMappedFixedValue` function makes the necessary spatial interpolations to map the precursor channel data to the room inlet boundary condition.

For the room simulations a complete study on grid independence was not performed, due to the long time necessary to perform the simulations. Instead of that, we decided to used a grid similar to that used in Ito et al. [5], i.e. a 210 x 63 x 296 (plus the inlet and outlet nodes) grid with a total of 3923280 cells, which is more than eight times the cells used by Almeida [4]. Simulations were performed for the four turbulence models until a steady state was achieved, that typically occur after near 500 seconds.

The numerical (steady state) results and experimental results for the 4 lines presented in Fig. 1b and at the symmetry plane are presented in Fig. 3. Globally the numerical results are in good agreement with the experimental results, with the exception of the predictions made by the $k - \omega SST$ model. This model overpredicted all recirculation zones when compared with either experimental results or the other turbulence models (see Fig. 4). All the other models produced a good description of the x-velocity field, along the vertical and horizontal lines of analysis. The turbulent intensity near the lower wall ($z = 0$) is less well predicted than at the wall jet (see Fig. 3b). The more difficult zone for the turbulence models was the vertical wall below the entrance, where the turbulent intensity was under-predicted by a large factor when compared with the experimental results (Fig. 3d), a problem already found in Almeida [4]. The agreement found in the plane $y = 2.7$ m (not shown) was identical to that found in the plane of symmetry ($y = 1.5$ m).

Taken all factors in consideration, it was decided to continue the validations tasks with the high-Reynolds number turbulence models, the $k - \epsilon$ and RNG $k - \epsilon$ models. The main reasons being the near wall mesh requirements imposed by the LaunderSharma $k - \epsilon$ model and the bad performance produced by the $k - \omega SST$ model in indoor spaces.

## 3 Murakami case study

To validate the numerical techniques and physical modeling of non-isothermal forced flows, the Murakami et al. [8] case study was used. In this second case study, the room is formed by a square air inlet ($L_0 = 0.04$ m) positioned in the center of a vertical wall, which will apply a cold air jet horizontally into the room ($30L_0 \times 20L_0 \times 20L_0$), extracting it through the opposite wall, through four square outlets ($L_0$) positioned at the corners of the heated wall (Fig. 5).

Following the conclusions of the first case study, only high-Reynolds number turbulence models were used,

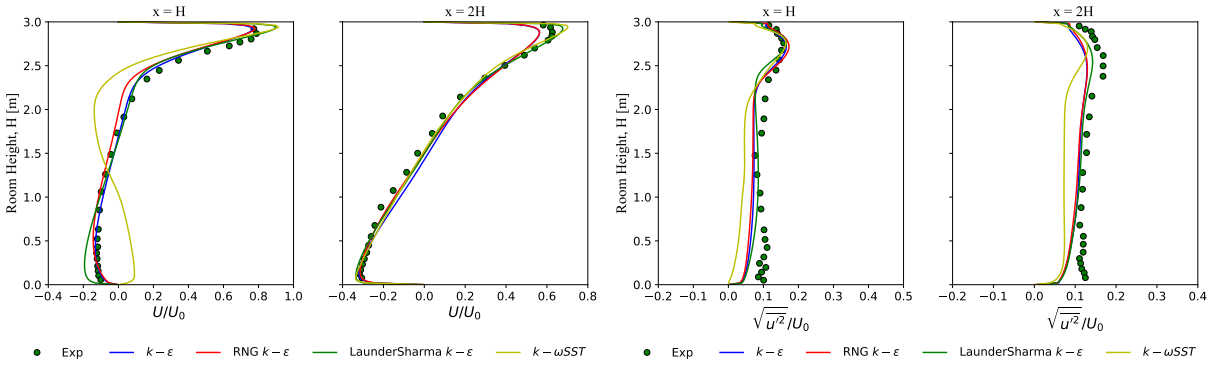


(a) Vertical profiles of velocity in the plane $y = 1.5$ m

(b) Vertical profiles of $TI$ in the plane $y = 1.5$ m

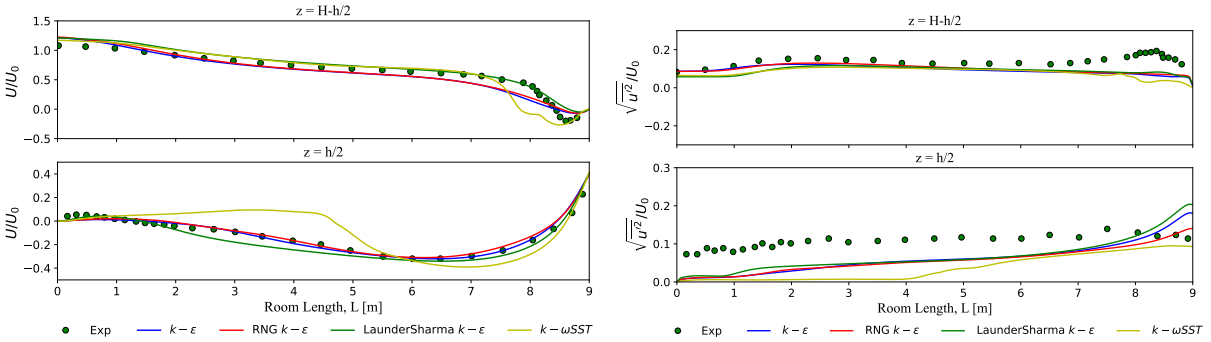


(c) Horizontal profiles of velocity in the plane $y = 1.5$ m

(d) Horizontal profiles of $TI$ in the plane $y = 1.5$ m

Figure 3. Annex 20 room results compared with experimental values from Nielsen [2]

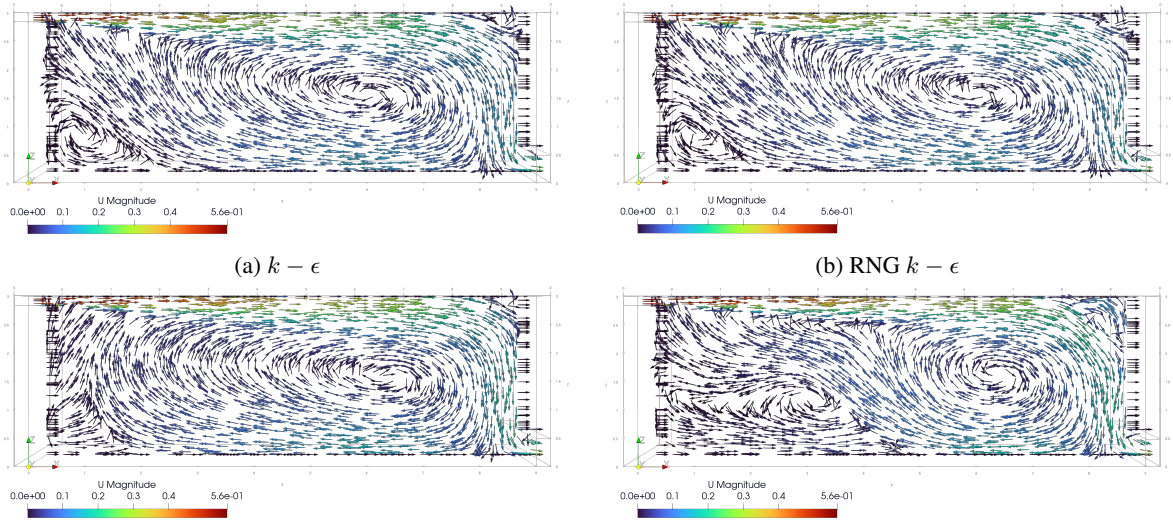


(a) $k-\epsilon$

(b) RNG $k-\epsilon$

(c) LaunderSharma $k-\epsilon$

(d) $k-\omega SST$

Figure 4. Velocity distributions in Annex 20

being these the $k-\epsilon$ with modeling of the buoyancy component (*buoyant* $k-\epsilon$) and isothermal $k-\epsilon$ and RNG $k-\epsilon$ models. The OpenFOAM `buoyantPimpleFoam` solver was used, which is a transient solver for buoyant, turbulent flows of compressible fluids for ventilation and heat-transfer applications. All simulations used `upwind` convection scheme. See OpenCFD [10], [11], Greenshields and Weller [12] for further details of models and solvers.

The velocity magnitude, U, temperature, $T$, and turbulent kinetic energy (TKE), $k$, were compared with the experimental measurements carried out with 3D ultrasonic anemometers by Murakami et al. [8] for the symmetry plane at $x/L_0 = 2.5$, $x/L_0 = 7.5$, $x/L_0 = 12.5$, $x/L_0 = 17.5$, $x/L_0 = 22.5$ and $x/L_0 = 27.5$.

In the study by Murakami et al. [8] several Archimedes numbers were used (eq. (1)) and the $Ar = 0.016$ was

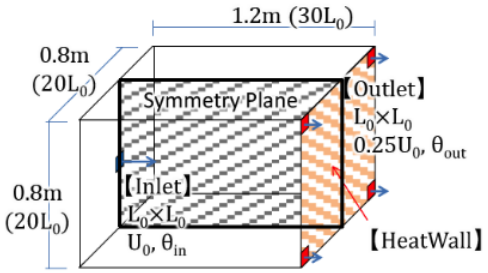


Figure 5. Scheme of Murakami's case study space, taken from Ito et al. [5]

chosen (case 5 model B of Murakami et al. [8]), as it is the most used case for numerical validation (e.g Ito et al. [5] and Murakami et al. [9]).

$$Ar = \frac{g\beta\Delta T_0 L_0}{U_0^2}. \tag{1}$$

For this $Ar$ number, $U_0 = 1$ m/s and the difference in temperature between the supply and exhaust air, $\Delta T_0 = 12°\text{C}$, was used to calculate the heat flux, $q''$, to be imposed on the extraction wall.

$$q'' = \frac{q}{A_{sur}}, \tag{2}$$

where $A_{sur}$ represents the area of the heated wall, without the area occupied by all four outlets and the heat rate, $q$, will be obtained by the thermal energy equation,

$$q = \dot{m} c_p \Delta T. \tag{3}$$

With these equations, the numerical value for the heat rate is $q = 23.98$ W resulting in a heat flux of $q'' = 37.85$ W/m$^2$, with all thermodynamic properties taken from a python implementation of the International Association for the Properties of Water and Steam (Wagner and Pruß [15]) for the outlet temperature (12.2°C). It should be noted that there is a slight difference between the calculated heat flux and the one by Murakami et al. [8] caused by small variations in the thermodynamic properties.

Mesh independence studies were carried out for a structured mesh and achieved with a grid of $70 \times 100 \times 106$ (plus the nodes in inlet and outlets), totalizing in 742125 CV. Simulations were carried until $\approx 700$ seconds, when a steady state was achieved.

Vertical profiles for the velocity magnitude, temperature and turbulent kinetic energy, using the three aforementioned turbulent models, are presented in Fig. 6.

Analysing the velocity results, it can be seen that the RNG $k-\epsilon$ produced the largest jet velocities, being this particularly noticeable for $x/L_0 = 7.5$ and 12.5. The sparsity of the experimental results doesn't allow to conclude which model produced a globally better description of the velocity field, with all the turbulence models showing a good agreement with experimental results.

In case of the temperature field, Fig. 6b, it can be seen that the buoyant $k-\epsilon$ gives the best results, particularly at locations further away from the inlet. It's near the top wall where all the three models struggled to follow the experimental results, with all models predicting higher temperatures. In this regard, the OpenFOAM results presented in Ito et al. [5] (not shown) follow more closely the experimental results near the heated wall and close the top wall, but with a globally cooler temperature field (worst agreement) than predicted in the present study.

The turbulent profiles, presented in Fig. 6c, showed that the buoyant $k-\epsilon$ and standard $k-\epsilon$ are almost indistinguishable, showing a better agreement with the experimental results, except in the two nearest locations to the inlet slot.

As a final conclusion it can be said that the present simulations produced a good agreement with the experimental results, and, as almost expected, the buoyant $k-\epsilon$ model had the best overall performance.

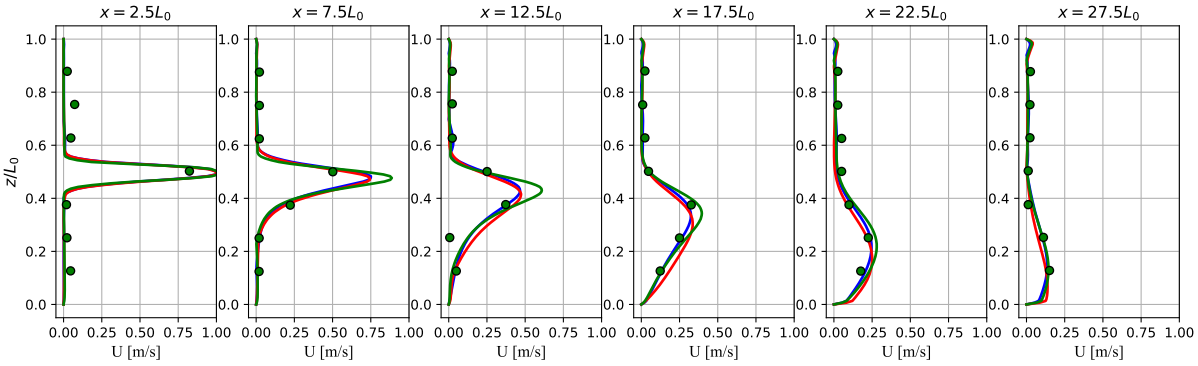


(a) Velocity magnitude

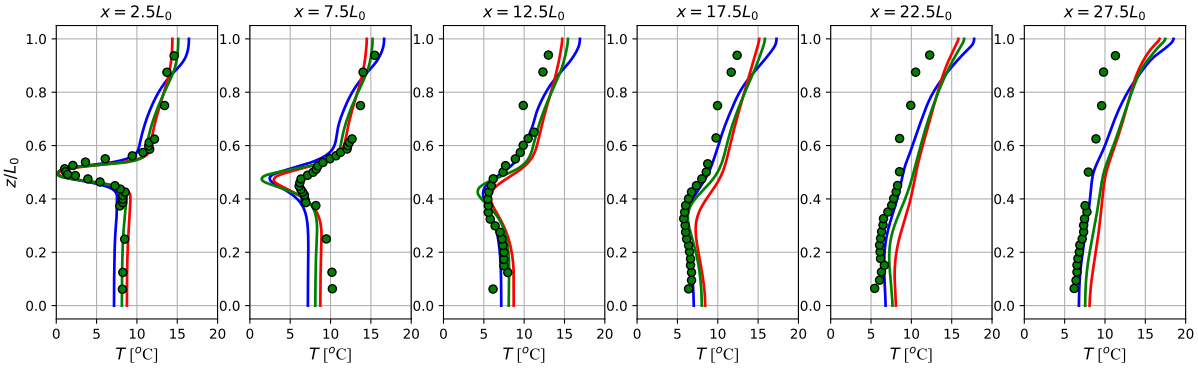


(b) Temperature

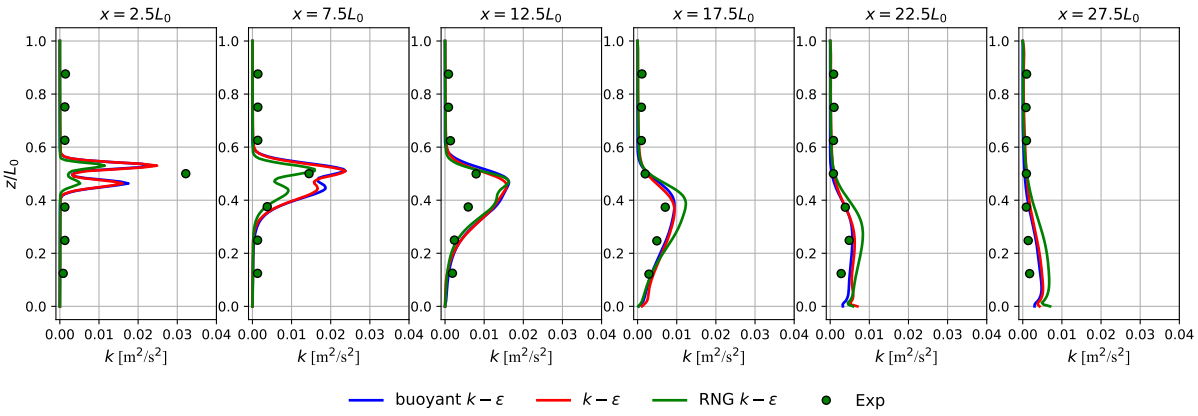


(c) Turbulent kinetic energy

Figure 6. Murakami et al. [8] case study results compared with the autor's own experimental values, taken from Ito et al. [5]

## 4 Conclusions

In this work we extended the work of Almeida [4] in the development of a numerical tool based in the OpenFOAM CFD software for the simulations of air distribution in rooms. For that purpose we resort to two well know experimental benchmarks.

In first case, Annex 20, we tested two high-Reynolds number models and two low-Reynolds number models. The results showed that despite the good performance of the $k-\omega SST$ in the precursor channel flow simulations, that were used to produce the inlet boundary condition for the room, it overpredicted the size of the flow recirculation in the room and can be considered the worst result of the tested turbulence models. After analysing all results it was decided to continue the validation tasks with the high-Reynolds number turbulence models, the $k-\epsilon$ and RNG $k-\epsilon$ models. The main reasons being the near wall mesh additional requirements imposed by the LaunderSharma $k-\epsilon$ model and as mentioned the bad performance produced by the $k-\omega SST$.

In the second case, a non-isothermal flow in a room with heated wall, the numerical results produced a good

description of the flow, irrespective of the turbulence model being used (buoyant $k-\epsilon$ and isothermal $k-\epsilon$ and RNG $k-\epsilon$). Nevertheless, the best results were obtained with the buoyant $k-\epsilon$ model especially on the temperature field near the heated wall, pointing the importance of the buoyant term inclusion on other popular turbulence models of the OpenFOAM library.

**Authorship statement.** The authors hereby confirm that they are the sole liable persons responsible for the authorship of this work, and that all material that has been herein included as part of the present paper is either the property (and authorship) of the authors, or has the permission of the owners to be included here.

## References

[1] M. González-Torres, L. Pérez-Lombard, J. F. Coronel, I. R. Maestre, and D. Yan. A review on buildings energy information: Trends, end-uses, fuels and drivers, 2022.
[2] P. V. Nielsen. Aalborg universitet specification of a two-dimensional test case (iea), 1990.
[3] A. Restivo. *Turbulent Flow in Ventilated Rooms*. PhD thesis, University of Londen, 1979.
[4] C. P. D. Almeida. Turbulence models study applied to indoor space ventilation, 2021.
[5] K. Ito, K. Inthavong, T. Kurabuchi, T. Ueda, T. Endo, T. Omori, H. Ono, S. Kato, K. Sakai, Y. Suwa, H. Matsumoto, H. Yoshino, W. Zhang, and J. Tu. Cfd benchmark tests for indoor environmental problems: Part 1 isothermal/non-isothermal flow in 2d and 3d room model, 2015.
[6] L. Rong and P. V. Nielsen. Aalborg universitet simulation with different turbulence models in an annex 20 room benchmark test using ansys cfx 11.0, 2008.
[7] B. Elhadidi and H. E. Khalifa. Comparison of coarse grid lattice boltzmann and navier stokes for real time flow simulations in rooms. *Building Simulation*, vol. 6, pp. 183–194, 2013.
[8] S. Murakami, S. Kato, and H. Nakagawa. Numerical and experimental study for flow and temperature fields in rooms with horisontal nonisothermal jets. *Journal of Architecture, Planning and Environmental Engineering*, pp. 11–21, 1991.
[9] S. Murakami, D. E. Member, A. S. Kato, and A. Y. Kondo. Numerical prediction of horizontal nonisothermal 3-d jet in room based on algebraic second-moment closure model, 1993.
[10] OpenCFD. Openfoam®: Open source cfd : Documentation.
[11] OpenCFD. Openfoam®: Open source cfd : Api.
[12] C. Greenshields and H. Weller. *Notes on Computational Fluid Dynamics: General Principles*. CFD Direct Ltd, 2022.
[13] A. E. Goltsman, I. A. Davletshin, N. I. Mikheev, and A. A. Paereliy. Shear stresses in turbulent pulsating channel flow. *Thermophysics and Aeromechanics*, vol. 22, pp. 319–328, 2015.
[14] S. B. Pope. *Turbulent Flows*. Cambridge University Press, 2000.
[15] W. Wagner and A. Pruß. The iapws formulation 1995 for the thermodynamic properties of ordinary water substance for general and scientific use. *Journal of physical and chemical reference data*, vol. 31, n. 2, pp. 387–535, 2002.